# Synthesis and characterization of $Na_5M(MoO_4)_4$ (M = Y,Yb) microwave ceramics for ULTCC applications

Johnson Dhanya, Elattuvalappil Kalathil Suresh, Rajaram Naveenraj, Ravendran Ratheesh

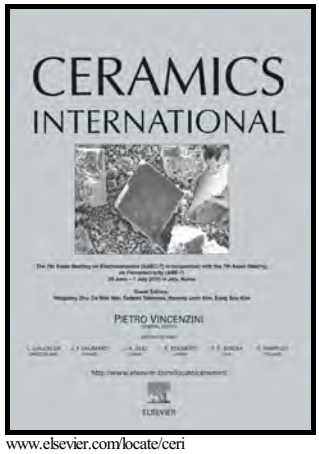


www.elsevier.com/locate/ceri

PII: S0272-8842(18)30096-8
DOI: https://doi.org/10.1016/j.ceramint.2018.01.084
Reference: CERI17216

To appear in: *Ceramics International*

Received date: 26 December 2017
Revised date: 10 January 2018
Accepted date: 11 January 2018

Cite this article as: Johnson Dhanya, Elattuvalappil Kalathil Suresh, Rajaram Naveenraj and Ravendran Ratheesh, Synthesis and characterization of $Na_5M(MoO_4)_4$ (M = Y,Yb) microwave ceramics for ULTCC applications, *Ceramics International,* https://doi.org/10.1016/j.ceramint.2018.01.084

# Synthesis and characterization of $Na_5M(MoO_4)_4$ (M = Y,Yb) microwave ceramics for ULTCC applications

Author list

**Johnson Dhanya[b], Elattuvalappil Kalathil Suresh[b], Rajaram Naveenraj[b] and Ravendran Ratheesh[a]***

[a]Centre for Materials for Electronics Technology (C-MET),
Ministry of Electronics and Information Technology, Government of India,
Hyderabad, Telangana, India- 500051

[b]Microwave Materials Division, Centre for Materials for Electronics Technology (C-MET),
Ministry of Electronics and Information Technology, Government of India,
Thrissur, Kerala, India-680581

*Corresponding author

Tel.: +91-040-27265673; fax: +91-040-27261658

E-mail address: ratheesh@cmet.gov.in

URL: http://www.cmet.gov.in

**Abstract**

$Na_5Y(MoO_4)_4$ and $Na_5Yb(MoO_4)_4$ ceramics are prepared by solid state ceramic route and structural characterization has been done using powder X-ray diffraction and Laser Raman spectroscopy techniques. The presence of $MoO_4^{2-}$ units in the crystal structure is confirmed from Raman spectra. The scanning electron micrographs of the sintered ceramic samples show dense microstructure. $Na_5Y(MoO_4)_4$ ceramics exhibited a maximum sintered density of 3.6 g/cm$^3$ at 600°C with a dielectric constant of 7.8, quality factor (Q × f) of 56,800 GHz, and temperature coefficient of resonant frequency ($\tau_f$) of -83 ppm/°C, whereas $Na_5Yb(MoO_4)_4$ ceramics showed a maximum sintered density of 3.9 g/cm$^3$ at 570°C with a dielectric constant of 6.9, quality factor (Q × f) of 43,400 GHz, and temperature coefficient of resonant frequency ($\tau_f$) of -68 ppm/°C. Powder X-ray diffraction and energy dispersive X-ray spectroscopic analyses of the co-fired samples confirm good chemical compatibility with aluminium electrode for $Na_5Yb(MoO_4)_4$ ceramics and hence is a suitable candidate material for ULTCC applications.

Keywords: A. Sintering, B. Electron microscopy, C. Dielectric properties, Raman spectroscopy.

## 1. Introduction

Low temperature co-fired ceramic (LTCC) technology is a multilayer circuit fabrication technique which facilitate integration of many circuit components into highly miniaturised systems [1-3]. LTCC technology has immense applications in wireless communication systems such as power amplifiers, radar devices, RF front end modules etc. [4-8]. LTCC technology involves the fabrication of green tapes from suitable ceramic powders followed by metallization using appropriate conducting paste formulations. Circuits are screen printed on green tapes, followed by stacking the thin dielectric layers and sintering them at appropriate temperatures [9-11].

The ceramic compositions used for LTCC systems should possess the following properties such as low sintering temperature (i.e. less than 960$^{o}$C) which is the melting point of silver, low dielectric constant, low dielectric loss, low temperature coefficient of resonant frequency, chemical compatibility with silver electrode on co-firing, appropriate thermal and mechanical properties etc. Ultra low temperature co-fired ceramics (ULTCC) are a new class of materials which can be sintered below 660$^{o}$C, where in aluminium paste is used as the metal electrode [1-3,12]. ULTCC technology enables better miniaturisation and cost reduction compared to LTCC packaging technology. Glass free LTCC and ULTCC compositions co-firable with both silver and aluminium metal electrodes reported largely in the literature comprise of molybdenum [13-18], tellurium [19-21] and vanadium [22-26] based oxide ceramics.

Recently a few sodium molybdate based compositions have been reported as suitable candidates for ULTCC applications [14,27]. In the present study, authors have intuitively revisited the phase diagram of $Na_2MoO_4$-$M_2(MoO_4)_3$ double molybdate with

Na:M ratio 5:1, where M represent yttrium and other rare earth ions. Mokhosoev et al. has reported the synthesis of $Na_5Ln(MoO_4)_4$ (Ln = La-Lu) by solid state ceramic route and correlated the lattice parameters with ionic radii [28,29]. Stedman et al. has reported the synthesis and detailed structural characterization of $Na_5Y(MoO_4)_4$ ceramics [30]. Though the series is reported to be isostructural with identical structural units, the bond lengths and molecular arrangements are varied with respect to the rare earth ion, which are attributed to the electronegativity differences in the trivalent cation in the composition [28-34]. In the present work, yttrium and a heavier rare earth ion ytterbium are chosen for a comparative evaluation of variation in their structural arrangements and associated changes in the microwave dielectric properties. The chemical compatibility of the material system with aluminium electrode is also studied at length.

$Na_5Y(MoO_4)_4$ and $Na_5Yb(MoO_4)_4$ ceramics have been prepared by solid state ceramic route. The structure and molecular structure of the compositions are studied using powder X-ray diffraction and laser Raman spectroscopic techniques. The microwave dielectric properties and chemical compatibility of the compositions with aluminium metal electrode are also investigated using XRD and energy dispersive X-ray spectroscopy with a view to use them for ultra-low temperature co-firable applications.

## 2. Materials and Methods

$Na_5Y(MoO_4)_4$ and $Na_5Yb(MoO_4)_4$ ceramics, (hereafter referred to as NYM and NYbM ceramics) were prepared by the conventional solid-state ceramic route. The starting materials used were $NaCO_3$ (99.9 %, Merck), $Y_2O_3$ (99.9 %, Star Rare Earth), $Yb_2O_3$ (99.9%, Treibacher) and $MoO_3$ (99%, Himedia). The stoichiometric proportions of these chemicals were accurately weighed and thoroughly mixed in an agate mortar using

double distilled water as the mixing medium. The resultant slurry was dried inside a hot air oven and calcined at 500 °C for 1 h in a programmable SiC furnace. The calcined powder was ground in an agate mortar into fine powder and 5 wt. % of polyvinyl alcohol (PVA) solution was added to it as binder and then dried. This fine powder was then made into cylindrical compacts using a 11 mm tungsten carbide die under a pressure of 200 MPa in a hydraulic hand press and sintered at temperatures in the range 560 to 610°C. The bulk density values of the sintered samples were determined accurately using Archimedes method using acetone as measuring medium.

Powder X-ray diffraction (XRD) measurement of the samples was carried out using Brucker AXS model X-ray diffractometer with CuKα radiation. The Raman spectra of the compositions under study were recorded using a Thermo Scientific DXR with Nd:$YVO_4$ DPSS laser of 532nm. The sintered samples were thermally etched for 30 min at a temperature of about 100ºC below the sintering temperature, and the surface morphology was studied using a scanning electron microscope (Carl Zeiss, Model No: EVO18 Research, Germany). The energy dispersive X-ray spectroscopy (EDS) technique was used for analysing the chemical compatibility of the ceramic samples with aluminium metal electrode. A Vector Network Analyser (Agilent make PNA E8362B, Bayan Lepas, Malaysia) was used to measure the microwave dielectric properties of the well sintered ceramics. The dielectric constant of the sample was measured by Hakki and Coleman post resonator technique [35] and the quality factor was measured by resonant cavity method (Krupka cavity) [36]. The temperature coefficient of resonant frequency '$\tau_f$' of the ceramics was also measured in the temperature range 30–100$^{o}$C.

**3. Results and discussion**

The X-ray diffraction patterns of NYM and NYbM ceramics are given in Fig. 1. The $Na_5Ln(MoO_4)_4$ series is reported to be isostructural for all rare earth ions and yttrium. The title compositions have tetragonal crystal structure with $I4_1/a$ space group and 4 formula units per unit cell [28-34]. The X-ray diffraction patterns are indexed on the basis of standard ICDD (International Centre for Diffraction Data) file no. 82-2368 for $Na_5Y(MoO_4)_4$ ceramic. The XRD analysis reveals that the compositions under study are phase pure as all the peaks are exactly matching with that of the standard ICDD data. The calculated lattice parameters obtained for NYM are a= 11.368Å and c= 11.427Å and the same for NYbM are a= 11.319Å and c=11.385Å. The XRD patterns of both Y and Yb analogues show similar features.

The laser Raman spectra of both NYM and NYbM ceramics are given in Fig. 2. The crystal structure of $Na_5Y(MoO_4)_4$ consists of molybdenum atom occupying the Wyckoff position 16(f) in the unit cell having approximately regular tetrahedral co-ordination with Mo-O bond lengths varying from 1.741 Å to 1.759 Å. The crystal structure also contains yttrium atoms occupying Wyckoff position 4(a) forming a slightly distorted $YO_8$ dodecahedron with two Y-O bond lengths 2.362 Å and 2.366 Å. The unit cell contains two types of Na atoms, of which one forms a regular $NaO_4$ tetrahedron and the other forms a highly irregular $NaO_6$ octahedron [30].

The four fundamental modes of vibration of $MoO_4^{2-}$, which include a non-degenerate symmetric stretching mode $\upsilon_1(A)$ at 894 $cm^{-1}$, a doubly degenerate symmetric bending mode $\upsilon_2(E)$ at 318 $cm^{-1}$, triply degenerate asymmetric stretching $\upsilon_3(F_2)$, and asymmetric bending $\upsilon_4(F_2)$ modes at 833 and 381 $cm^{-1}$, respectively are observed in the laser Raman spectra of both NYM and NYbM ceramics [37-40]. The symmetric stretching vibrations ($\upsilon_1$) of $MoO_4^{2-}$ tetrahedra are observed as a very strong peak at 917 $cm^{-1}$

together with weak shoulder at 937 $cm^{-1}$ for both the compositions. Prominent bands observed in the range 807 to 874 $cm^{-1}$ corresponds to the asymmetric stretching vibrations of $MoO_4^{2-}$ ions. The symmetric ($\upsilon_2$) bending vibrations of $MoO_4^{2-}$ tetrahedra are observed at 329 $cm^{-1}$ and 332 $cm^{-1}$ for NYM and NYbM ceramics respectively. The asymmetric ($\upsilon_4$) bending vibrations of $MoO_4^{2-}$ tetrahedra appear at 374 and 392 $cm^{-1}$ for NYM and 377 and 394 $cm^{-1}$ for NYbM ceramics respectively. The lattice-mode vibrations are observed below 250 $cm^{-1}$ and unambiguous assignment of these modes are difficult. Less number of vibrational modes observed in the symmetric and asymmetric stretching vibrations of $MoO_4^{2-}$ ions in both NYM and NYbM ceramics confirm a regular tetrahedral arrangement as proposed in the crystal structure studies by Stedman et al. [30].

Laser Raman spectra of both NYM and NYbM ceramics show similar vibrational features and hence it can be concluded that the molecular arrangements is the same for both the ceramics.

The SEM micrographs of NYM and NYbM ceramics sintered at 600°C and 570°C for 1 h are shown in Fig. 3(a) and (b). Both the samples show dense microstructure with polygonal grains of sizes 1 to 3 μm which are evenly distributed.

NYM and NYbM ceramics are sintered at various temperatures in the range 560°C to 610°C for 1 h to obtain maximum density. The variation of density with sintering temperature for NYM and NYbM ceramics are shown in Fig. 4. NYM ceramic shows a maximum sintered density of 3.6 $g/cm^3$ with 95 % densification at 600°C, with dielectric constant ($\varepsilon_r$) of 7.8, quality factor (Q × f) of 56,800 GHz, and temperature coefficient of resonant frequency ($\tau_f$) of -83 ppm/°C. Whereas, NYbM ceramic shows a maximum sintered density of 3.9 $g/cm^3$ with 93% densification at 570°C, with dielectric constant

($\varepsilon_r$) of 6.9, quality factor (Q × f) of 43,400 GHz, and temperature coefficient of resonant frequency ($\tau_f$) of -68 ppm/°C. The lower dielectric constant for NYbM ceramic is attributed to the lower ionic polarizability value for Ytterbium 3.58 $Å^3$ compared to 3.81 $Å^3$ for Yttrium [41].

The variation of resonant frequency with temperature of NYM ceramic sintered at 600°C/1h and that of NYbM ceramic sintered at 570°C/1h is shown in Fig. 5.

The chemical compatibility of NYM and NYbM ceramics with aluminium electrode is studied by powder X-ray diffraction and energy dispersive X-ray spectroscopy (EDS) analyses of ceramic samples co-fired with 20 wt. % of aluminium powder at 600°C for 1 h and 570°C for 1 h respectively. The XRD patterns of the co-fired samples are shown in Fig. 6(a) and 6(b). Compared to co-fired NYM sample, the XRD pattern of NYbM ceramic co-fired with aluminium exhibits well defined peaks of aluminium at 2θ values 38.5°, 44.7° and 65.1°, marked with '*', in addition to the characteristic peaks of the ceramics. The backscattered SEM images of the co-fired sample, elemental colour mapping and the EDS point analysis done separately at aluminium region (spot 1) and ceramic region (spot 2) for NYM ceramic are shown in Fig. 7(a-d) and that of NYbM ceramic are shown in Fig. 8(a-d). The EDS line scan of NYbM ceramic is shown in Fig. 9.The phase map of both the samples show co-fired aluminium as an island surrounded by the sintered ceramic. However, the EDS point analysis at the aluminium region in the co-fired NYM sample shows traces of the ceramic phase also, which indicates possible reaction between the ceramic and aluminium phases. Whereas, in the case of co-fired NYbM ceramic, EDS point analysis shows the presence of metal aluminium only, which clearly indicates that Ytterbium composition exhibits better co-firability with aluminium electrode material. Due to 4f shell contraction, $Yb^{3+}$ ion in $YbO_8$

dodecahedron has lower ionic radii of 98 pm compared to 102 pm of $Y^{3+}$ ion in $YO_8$ dodecahedron and eight co-ordinated Yb-O bond is reported to be stronger than the Y-O bond. The lower sintering temperature for NYbM sample and relatively higher strength of Yb-O bond in the structure could be the possible reasons for the excellent compatibility of NYbM composition with Al metal [42].

## 4. Conclusions

NYM and NYbM ceramics have been prepared by solid state ceramic route. The structural characterization of the samples under study are carried out by powder X-ray diffraction. The molecular arrangements in the unit cell of the ceramics have been studied using laser Raman spectroscopy. The existence of regular $MoO_4^{2-}$ tetrahedral ions in the unit cells of both the compositions under study is confirmed through Raman studies. The scanning electron microscopic studies reveal that the microstructure of the sintered ceramic compacts are dense in nature with grain size ranging from 1 to 3 μm. NYM ceramic exhibited a dielectric constant of 7.8, quality factor (Q × f) of 56,800 GHz, and temperature coefficient of resonant frequency ($\tau_f$) of -83 ppm/°C whereas a dielectric constant ($\varepsilon_r$) of 6.9, quality factor (Q × f) of 43,400 GHz, and temperature coefficient of resonant frequency ($\tau_f$) of -68 ppm/°C are obtained for NYbM ceramic. Powder X-ray diffraction and energy dispersive X-ray spectroscopy analyses of the ceramic samples co-fired with 20 wt. % aluminium show excellent chemical compatibility with the metal electrode for NYbM ceramic. Present study shows that $Na_5Yb(MoO_4)_4$ ceramic is an ideal candidate material for ULTCC applications.

**Acknowledgements**

The authors are grateful to Dr. N. Raghu, Director, C-MET, Thrissur for extending the facilities to the work. The authors are also thankful to the Board of Research in Nuclear Sciences, Mumbai for financial support under grant number 34/15/01/2014-BRNS/0906.

**References**

[1] J. Zhou, Towards rational design of low-temperature co-fired ceramic (LTCC) materials, J. Adv. Ceram. 1 (2012) 89–99.

[2] M.T. Sebastian, H. Jantunen, Low loss dielectric materials for LTCC applications: a review, Int. Mater. Rev. 53 (2008) 57–90.

[3] M.T. Sebastian, H. Wang, H.Jantunen, Low temperature co-fired ceramics with ultra-low sintering temperature: A review, Curr. Opin.Solid State Mater. Sci. 20 (2016) 151–170.

[4] D. Heo, A. Sutono, E. Chen, Y. Suh, J. Laskar, A 1.9-GHz DECT CMOS power amplifier with fully integrated multilayer LTCC passives, IEEE Microw. Compon.Lett. 11 (2001) 249–251.

[5] A. Sutono, D.Heo, Y.-J.E. Chen, J. Laskar, High-Q LTCC-based passive library for wireless system-on-package (SOP) module development, IEEE Trans. Microw. Theory Techn. 49 (2001) 1715–1724.

[6] F. Bauer, X. Wang, W. Menzel, A. Stelzer, A 79-GHz Radar Sensor in LTCC Technology Using Grid Array Antennas, IEEE Trans. Microw. Theory Techn. 61 (2013) 2514–2521.

[7] J.H. Lee, N. Kidera, G. DeJean, S. Pinel, J. Laskar, M.M. Tentzeris, A V-band front-end with 3-D integrated cavity filters/duplexers and antenna in LTCC technologies, IEEE Trans. Microw. Theory Techn. 54 (2006) 2925–2936.

[8] D.H. Kim, D. Kim, J.C Kim, C. D. Park, A novel single- band RF front- end module for wireless communication systems, Microw. Opt. Technol. Lett. 53 (2011) 1349–1352.

[9] M. Jabbari, R. Bulatova, A.I.Y.Tok, C.R.H.Bahl, E.Mitsoulis, J.H.Hattel, Ceramic tape casting: A review of current methods and trends with emphasis on rheological behaviour and flow analysis, Mater. Sci. Eng.,B 212 (2016) 39–61.

[10] K. Malecha, T. Maeder, C. Jacq, Fabrication of membranes and microchannels in low-temperature co-fired ceramic (LTCC) substrate using novel water-based sacrificial carbon pastes, J. Eur. Ceram. Soc. 32 (2012) 3277–3286.

[11] Y. Wang, G. Zhang, J. Ma,Research of LTCC/Cu, Ag multilayer substrate in microelectronic packaging,Mater. Sci. Eng.,B 94 (2002) 48–53.

[12] H. Yu, J. Liu, W. Zhang, S. Zhang, Ultra-low sintering temperature ceramics for LTCC applications: a review, J. Mater. Sci. - Mater.Electron. 26 (2015) 9414–9423.

[13] N. Joseph, J. Varghese, T. Siponkoski, M. Teirikangas, M.T. Sebastian, H. Jantunen, Glass-free $CuMoO_4$ ceramic with excellent dielectric and thermal properties for ultralow temperature cofired ceramic applications, ACS Sustain. Chem. Eng. 4 (2016) 5632–5639.

[14] J. Dhanya, A.V. Basiluddeen, R. Ratheesh, Synthesis of ultra low temperature sinterable $Na_2Zn_5(MoO_4)_6$ ceramics and the effect of microstructure on microwave dielectric properties, Scripta Mater. 132 (2017) 1–4.

[15] A. Surjith, E.K. Suresh, S. Freddy, R. Ratheesh, Microwave dielectric properties of low temperature sinterable $RE_2Mo_4O_{15}$ (RE= Nd, Sm) ceramics for LTCC applications, J. Mater. Sci. - Mater.Electron. 24 (2013) 1818–1822.

[16] D. Zhou, C.A. Randall, L.X. Pang, H. Wang, X.G. Wu, J. Guo, G.Q. Zhang, L. Shui, X. Yao, Microwave Dielectric Properties of $Li_2$ $(M^{2+})_2Mo_3O_{12}$ and $Li_3$ $(M^{3+})Mo_3O_{12}$ (M= Zn, Ca, Al, and In) Lyonsite- Related- Type Ceramics with Ultra- Low Sintering Temperatures, J. Am. Ceram. Soc. 94 (2011) 802–805.

[17] D.Zhou, C.A.Randall, A.Baker, H.Wang, L.X.Pang, X.Yao, Dielectric Properties of an Ultra- Low- Temperature Cofiring $Bi_2Mo_2O_9$ Multilayer, J. Am. Ceram. Soc. 93 (2010) 1443–1446.

[18] D.Zhou, C.A. Randall, H. Wang, L.X.Pang, X.Yao, Microwave Dielectric Ceramics in $Li_2O$–$Bi_2O_3$–$MoO_3$ System with Ultra- Low Sintering Temperatures, J. Am. Ceram. Soc. 93 (2010) 1096–1100.

[19] D.K.Kwon, M.T.Lanagan, T.R.Shrout, Synthesis of $BaTiTe_3O_9$ ceramics for LTCC application and its dielectric properties, J. Ceram. Soc. Jpn. 113 (2005) 216–219.

[20] G.Subodh, M.T.Sebastian, Glass- Free $Zn_2Te_3O_8$ Microwave Ceramic for LTCC Applications, J. Am. Ceram. Soc. 90 (2007) 2266–2268.

[21] J. Honkamo, H. Jantunen, G. Subodh, M.T. Sebastian, P. Mohanan, Tape Casting and Dielectric Properties of $Zn_2Te_3O_8$- Based Ceramics with an Ultra- Low Sintering Temperature, Int. J. Appl. Ceram. Technol. 6 (2009) 531–536.

[22] E.K. Suresh, A.N.Unnimaya, A. Surjith, R. Ratheesh, New vanadium based $Ba_3MV_4O_{15}$ (M = Ti, and Zr) high Q ceramics for LTCC applications, Ceram. Int. 39 (2013) 3635–3639.

[23] A.N.Unnimaya, E.K.Suresh, R. Ratheesh, Crystal structure and microwave dielectric properties of new alkaline earth vanadate $A_4V_2O_9$ (A= Ba, Sr, Ca, Mg and Zn) ceramics for LTCC applications, Mater. Res. Bull. 88 (2017) 174–181.

[24] E.K. Suresh, K. Prasad, N.S. Arun, R. Ratheesh, Synthesis and microwave dielectric properties of $A_{16}V_{18}O_{61}$ (A= Ba, Sr and Ca) ceramics for LTCC applications, J. Electron. Mater.45 (2016) 2996–3002.

[25] E.K. Suresh, A.N. Unnimaya, R. Ratheesh, Microwave Dielectric Properties of Ultralow- Temperature Cofirable $Ba_3V_4O_{13}$ Ceramics, J. Am. Ceram. Soc. 97 (2014) 1530–1533.

[26] A.N. Unnimaya, E.K. Suresh, R. Ratheesh, Structure and microwave dielectric properties of ultralow-temperature cofirable $BaV_2O_6$ ceramics, Eur. J. Inorg. Chem. 2 (2015) 305–310.

[27] G.-Q. Zhang, H. Wang, J. Guo, L. He, D.-D.Wei, Q.-B. Yuan, Ultra-low sintering temperature microwave dielectric ceramics based on $Na_2O$–$MoO_3$ binary system, J. Am. Ceram. Soc. 98 (2015) 528–533.

[28] M.V. Mokhosoev, F.P. Alekseev, E.I.Get'man, Double molybdates of the rare-earth elements and sodium of composition $Na_5Ln(MoO_4)_4$, Russ. J. Inorg. Chem. 14 (1969) 310-311.

[29] M.V. Mokhosoev, I.F. Kokot, V.I. Lutsyk, I.S. Kononenko, Interaction in melts between double lanthanum alkali metal molybdates and alkali metal molybdates, Russ. J. Inorg. Chem. 15 (1970) 142–144.

[30] N.J. Stedman, A.K. Cheetham, P.D. Battle, Crystal structures of two sodium yttrium molybdates: NaY $(MoO_4)_2$ and $Na_5Y(MoO_4)_4$, J. Mater. Chem. 4 (1994) 707-711.

[31] V.A. Efremov, T.A. Berezina, I.M. Averina, V.K. Trunov, Structure of $Na_5Tb(MoO_4)_4$, $Na_5Lu(MoO_4)_4$, and $Na_5Lu(WO_4)_4$, Sov. Phys. Crystallogr. 25 (1980) 146–150.

[32] V. A. Efremov, V.K. Trunov, T.A. Berezina, Fine changes in the structure of scheelite-like $Na_5TR(EO_4)_4$ with a variation in their elemental composition, Sov. Phys. Crystallogr. 27 (1982) 77–81.

[33] V.K. Trunov, T.A. Berezina, A.A. Evdokimov, V.K. Ishunin, V.G.Krongauz, Sodium rare-earth-element double molybdates and tungstates, Russ. J. Inorg. Chem. 23 (1978) 1465-1467.

[34] R.F. Klevtsova, L.A. Glinskaya, L.P. Kozeeva, P.V. Klevtsov, The double sodium lutetium tungstates, $NaLu(WO_4)_2$ and $Na_5Lu(WO_4)_4$ and their crystal structures, Sov. Phys. Crystallogr. 17 (1973) 672–676.

[35] B.W. Hakki, P.D. Coleman, A dielectric resonator method of measuring inductive capacities in the millimeter range, IRE Trans. Microwave Theory Tech. 8 (1960) 402–410.

[36] J. Krupka, K. Derzakowski, B. Riddle, J.B. Jarvis, A dielectric resonator for measurements of complex permittivity of low loss dielectric materials as a function of temperature, Meas. Sci. Technol. 9 (1998) 1751–1756.

[37] F.D. Hardcastle, I.E. Wachs, Molecular structure of molybdenum oxide in bismuth molybdates by Raman spectroscopy, J. Phys. Chem. 95 (1991) 10763–10772.

[38] F.D. Hardcastle, I.E. Wachs, Determination of molybdenum–oxygen bond distances and bond orders by Raman spectroscopy, J. Raman Spectrosc. 21 (1990) 683–691.

[39] N.K. James, R. Ratheesh, Microwave Dielectric Properties of Low- Temperature Sinterable $BaCe_2(MoO_4)_4$ Ceramics, J. Am. Ceram. Soc. 93 (2010) 931-933.

[40] A. Surjith, R. Ratheesh, High Q Ceramics in the $ACe_2(MoO_4)_4$(A = Ba, Sr and Ca) System for LTCC applications, J. Alloys Compd. 550 (2013) 169–172.

[41] R. D. Shannon, Dielectric Polarizabilities of Ions in Oxides and Fluorides, J. Appl. Phys. 73 (1993) 348–366.

[42] Y.C. Zhou, H.M. Xiang, Z.H. Feng, Theoretical investigation on mechanical and thermal properties of a promising thermal barrier material: $Yb_3Al_5O_{12}$, J. Mater. Sci. Technol. 30 (2014) 631−638.

**Figure captions**

Fig. 1. XRD patterns of (a) $Na_5Y(MoO_4)_4$ ceramics sintered at 600°C for 1h; (b) $Na_5$ Yb $(MoO_4)_4$ ceramics sintered at 570°C for 1h.

Fig. 2. Laser Raman spectra of (a) $Na_5Y(MoO_4)_4$ ceramics sintered at 600°C for 1h; (b) $Na_5$ Yb$(MoO_4)_4$ ceramics sintered at 570°C for 1h.

Fig. 3. SEM micrographs of (a) $Na_5Y$ $(MoO_4)_4$ ceramics sintered at 600°C for 1h; (b) $Na_5$ Yb $(MoO_4)_4$ ceramics sintered at 570°C for 1h.

Fig. 4. Sintered density as a function of sintering temperature for $Na_5Y(MoO_4)_4$and $Na_5Yb(MoO_4)_4$ ceramics.

Fig. 5. Temperature variation of resonant frequency for $Na_5Y(MoO_4)_4$ ceramic sintered at 600°C for 1 h and $Na_5Yb(MoO_4)_4$ ceramic sintered at 570°C for 1 h.

Fig. 6. XRD patterns of (a) $Na_5Y(MoO_4)_4$ ceramic co-fired with 20 wt. % Al at 600°C for 1 h.; (b) $Na_5Yb(MoO_4)_4$ ceramic co-fired with 20 wt.% Al at 570°C for 1 h.

Fig. 7. (a) SEM image of $Na_5Y(MoO_4)_4$ ceramic with 20 wt.% Al sintered at 600°C for 1 h; (b) Elemental colour mapping of the $Na_5Y(MoO_4)_4$ ceramic sintered with 20 wt.% Al; (c) EDS spectrum at spot 1 (d) EDS spectrum at spot 2.

Fig. 8. (a) SEM image of $Na_5Yb(MoO_4)_4$ ceramic with 20 wt.% Al sintered at 570°C for 1 h; (b) Elemental colour mapping of the $Na_5Yb(MoO_4)_4$ ceramic sintered with 20 wt.% Al; (c) EDS spectrum at spot 1 (d) EDS spectrum at spot 2.

Fig. 9. Line scan image of $Na_5Yb(MoO_4)_4$ ceramic with 20 wt.% Al sintered at 570°C for 1 h.

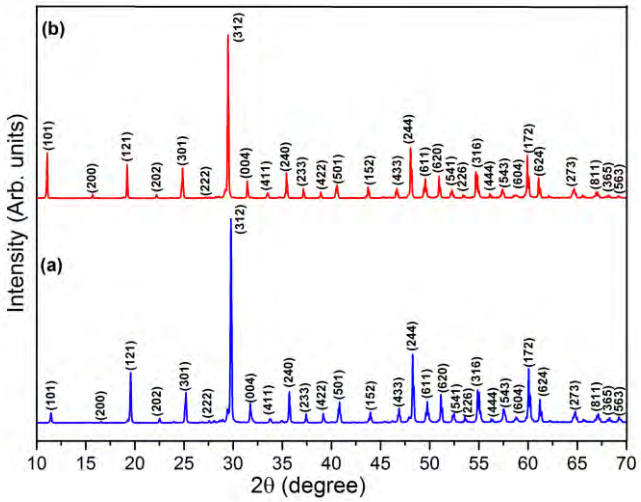


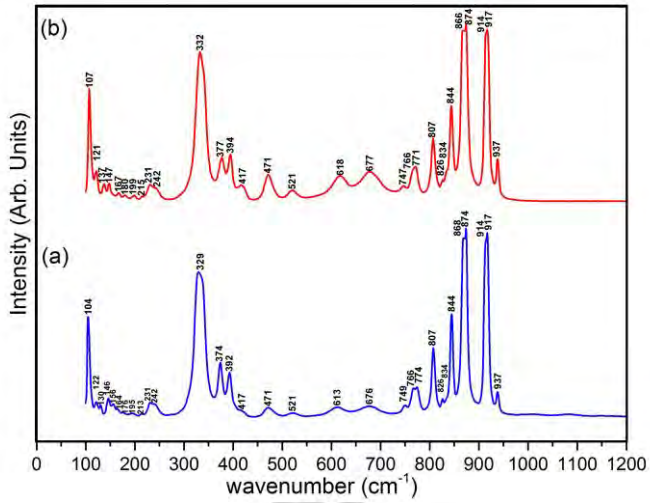


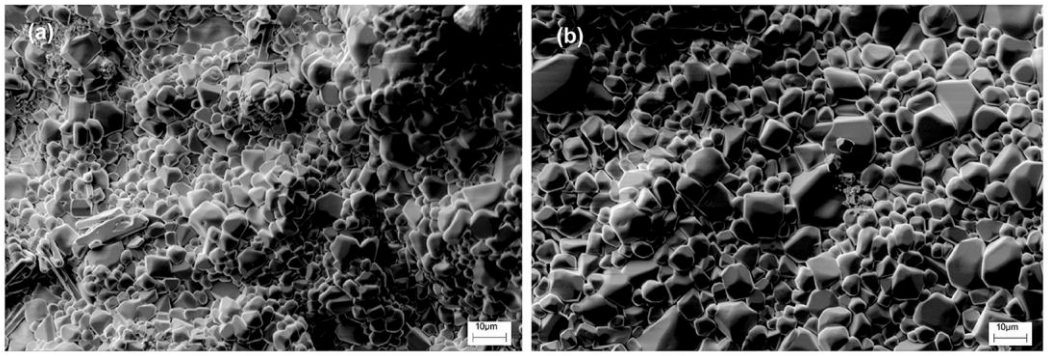

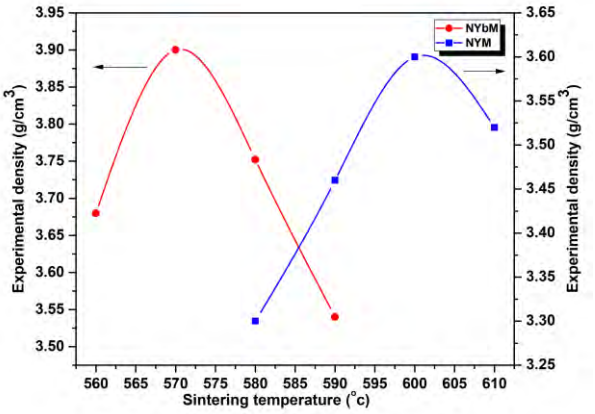


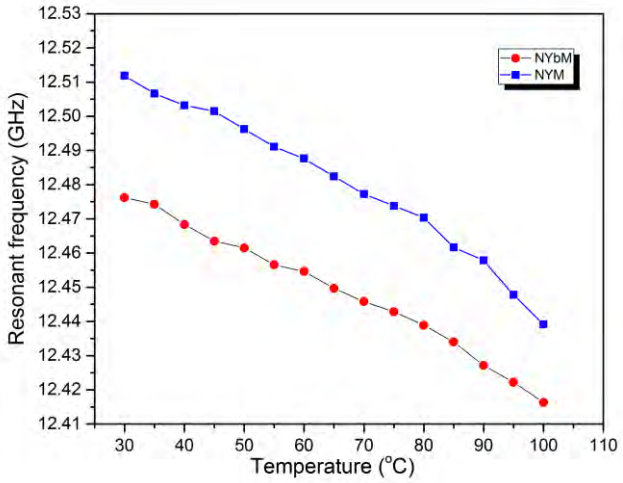

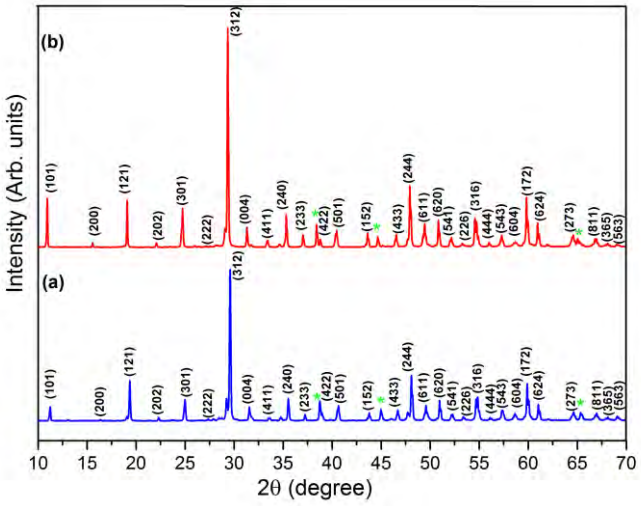


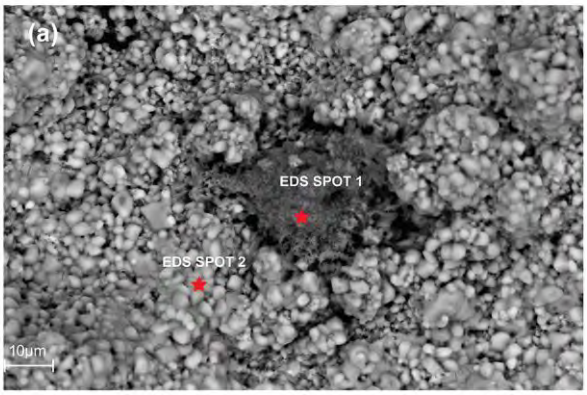


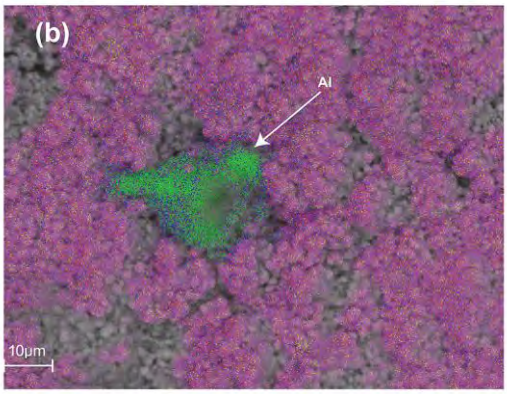


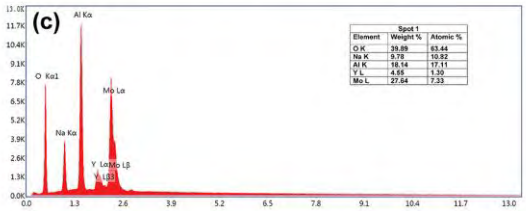


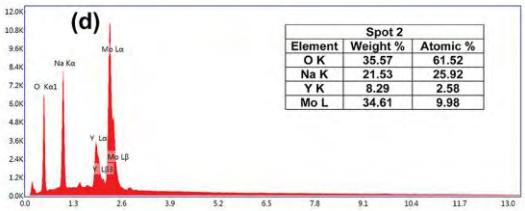


Spot 2

| Element | Weight % | Atomic % |
|---|---|---|
| O K | 35.57 | 61.52 |
| Na K | 21.53 | 25.92 |
| Y K | 8.29 | 2.58 |
| Mo L | 34.61 | 9.98 |